The Effect of Diphenylethane Side-chain Substituents on Dibenzocyclohexadiene Formation and their Inhibition of α-Synuclein Aggregation *in vitro*

Gabriel Da Silva, Omer Munir, Ed S. Krol*

Drug Discovery and Development Research Group, College of Pharmacy and Nutrition, University of Saskatchewan, Saskatoon, SK

 *Author to whom correspondence should be addressed

Dr. Ed S. Krol

Drug Discovery and Development Research Group

College of Pharmacy and Nutrition

University of Saskatchewan

Saskatoon, SK

Ph: 306-966-2011

ed.krol@usask.ca

Keywords

Di-catechol diphenylethanes; dibenzocyclohexadienes; in vitro alpha-synuclein aggregation;

oxidative instability; intramolecular cyclization; vicinal dimethyl effect; geminal dimethyl effect

Abbreviations

NDGA, nordihydroguaiaretic acid; GSH, reduced glutathione; PBS, Phosphate buffered saline;

MMPPD, 2,2-di-(3-methoxymethylphenyl)-1,3-propanediol; cNDGA, cyclized NDGA; NMR,

nuclear magnetic resonance; DPE, 4,4'-(ethane-1,2-diyl)bis(benzene-1,2-diol); M2-DPE, 2,3-

Bis(3,4-dihydroxyphenyl)butane; M4-DPE, 4,4'-(2,3-dimethylbutane-2,3-diyl)bis(benzene-1,2-

diol); PIFA, bis(trifluoroacetoxy)iodobenzene; o-DPE A, 2,3,6,7-tetrahydroxy-9,10-dihydrophenanthrene; o-DPE B, 2,3,6,7-tetrahydroxy-9,10-dihydrophenanthrene; o-DPE C, 2,3,5,6-tetrahydroxy-9,10-dihydrophenanthrene; o-M2-DPE A, 2,3,6,7-tetrahydroxy-9,10-dimethylphenanthrene; o-M2-DPE B, 2,3,5,6-tetrahydroxy-9,10-dimethylphenanthrene; o-M4-DPE A, 2,3,6,7-tetrahydroxy-9,9,10,10-tetramethylphenanthrene; o-M4-DPE B, 2,3,5,6-tetrahydroxy-9,9,10,10-tetramethylphenanthrene; AS, α-synuclein; ANOVA, analysis of variance; ThT, Thioflavin T; DFT, Density Functional Theory.

1. Abstract

The naturally-occurring di-catechol lignan nordihydroguaiaretic acid (NDGA) and an analog without methyl groups on the butyl linker both undergo intramolecular cyclization at pH 7.4 to form dibenzocyclooctadienes. Both NDGA and these dibenzocyclooctadienes have been shown to prevent *in vitro* aggregation of α-synuclein, an intrinsically disordered protein associated with Parkinson's disease. NDGA possesses two vicinal methyl groups on the butyl linker and the presence of these methyl groups attenuates the rate of intramolecular cyclization versus the unsubstituted analog, in opposition to the anticipated Thorpe-Ingold effect, likely due to steric repulsions during cyclization.

Numerous 1,2-bis-ethane di-catechols are known to inhibit α-synuclein aggregation *in vitro* and we hypothesize that these compounds undergo a similar intramolecular cyclization and the cyclized products may be responsible for the activity. To test this hypothesis we prepared a series of 1,2-bis-ethane di-catechols with 0, 2 and 4 methyl substituents on the linker. We have confirmed that these compounds undergo intramolecular cyclization to form dibenzocyclohexadienes and that

steric interactions between the methyl substituents leads to an increase in the rate of intramolecular cyclization, which is in contrast to what was observed for lignan di-catechols. The rate of cyclization to form six-membered rings is 10-30 times more rapid than formation of eight membered rings and the dibenzocyclohexadienes also prevent *in vitro* aggregation of α-synuclein.

2. Introduction

Many natural products with reported pharmacological activity *in vivo* have been studied in *in vitro* systems in an effort to better understand their mechanisms of action at the biochemical level and provide screening methods for carrying out structure-activity studies. A concern over this approach is the instability of many natural products when exposed to *in vitro* systems. Curcumin has been suggested to possess a range of pharmacological properties [1–6], yet it's *in vivo* metabolic fate of reduction and phase 2 metabolism [7,8] is divergent from its known instability *in vitro* [9,10] which results in an oxidative rearrangement to produce a dioxygenated bicyclopentadione. Other natural products including flavonols and catechins have reported similar *in vitro* instabilities which differ from their *in vivo* metabolism [11,12]. We previously reported that the lignan nordihydroguaiaretic acid (NDGA, Figure 1) undergoes oxidative intramolecular cyclization to a dibenzocyclooctadiene in phosphate buffer [13], as does an analog which does not possess methyl groups on the alkyl linker (de-Me-NDGA), and that the presence of catechols on both aromatic rings is a requirement for intramolecular cyclization [14]. We recently showed that NDGA, de-Me-NDGA and their cyclized forms are able to prevent the *in vitro* aggregation of α-synuclein [15], an intrinsically misfolded protein whose aggregation has been associated with the pathophysiology of Parkinson's disease [16,17]. Interestingly, the presence of reducing agents which prevent oxidation/ cyclization attenuate the anti-aggregation effect. There have been previous reports of the potential for NDGA to treat neurological conditions *in vitro* [18,19] and we hypothesize that this may be due to formation of the dibenzocyclooctadiene during *in vitro* incubation.

A report on a series of substituted 1,2-bis-ethane di-catechols that were demonstrated to inhibit α-synuclein aggregation *in vitro* [20] led us to speculate that these compounds may undergo

autoxidative intramolecular cyclization to dibenzocyclohexadienes. To address the question of the generality of this oxidative process led us to investigate whether di-catechols with shorter linker chains than NDGA would also undergo similar intramolecular cyclizations, specifically focusing on the formation of six-membered ring dibenzocyclohexadienes. We hypothesized that *in vitro* autoxidation/ intramolecular cyclization of the 1,2-bis-ethane di-catechols may be associated with their α-synuclein anti-aggregation properties. Although we found evidence in the literature of dibenzocyclohexadienes, they were formed through processes other than oxidative cyclization of a di-catechol [21]. In addition, we had previously noted that the rate of cyclization for de-Me-NDGA (Figure 1), which does not possess methyl groups on the linker is more rapid than for NDGA. We had originally anticipated that the presence of methyl groups on the linker would enhance cyclization as a result of a Thorpe-Ingold effect [22], however our results suggested that steric interactions between the vicinal methyl groups during cyclization may rather impede this process [14]. Our goals are to prepare a series of 1,2-bis-ethane di-catechols with 0, 2 or 4 methyl groups on the alkyl linker in order to probe intramolecular cyclization products, rate of cyclization and ability to inhibit *in vitro* α-synuclein aggregation.
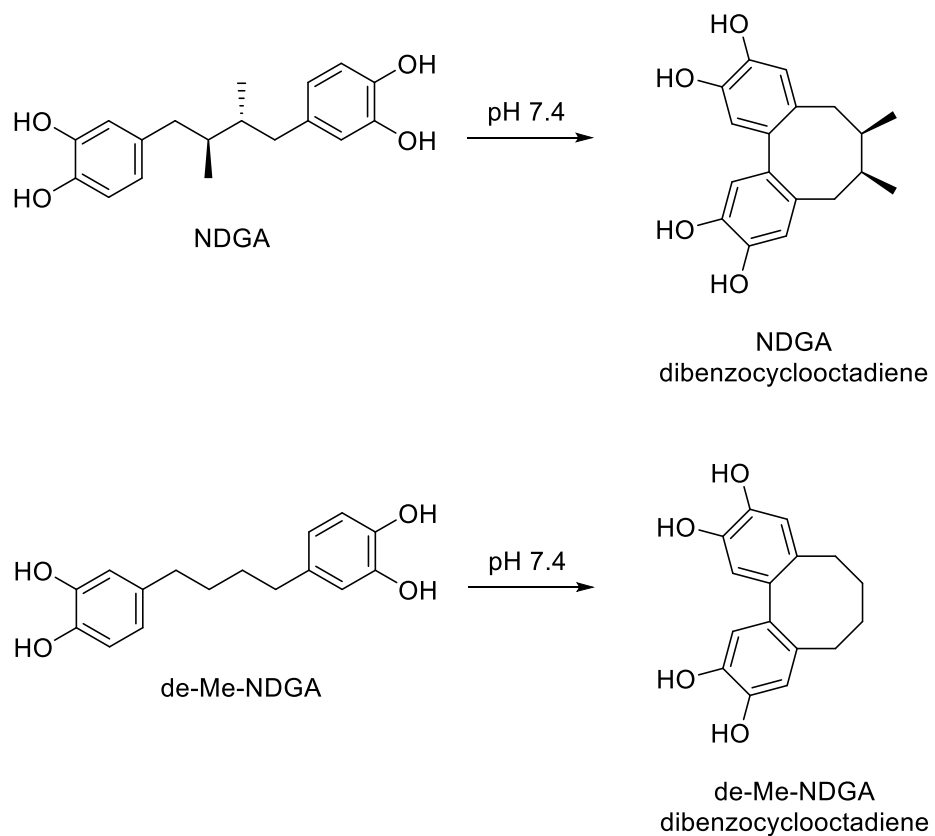
Figure 1. Structures of NDGA (2 methyl groups on the alkyl linker) and de-Me-NDGA (0 methyl groups on the alkyl linker) and their respective dibenzocyclooctadienes formed via intramolecular cyclization.

3. Materials and Methods

3.1 Materials

Reduced glutathione (GSH), Thioflavin T, Phosphate buffered saline (PBS), K_2HPO_4 were purchased from Sigma-Aldrich while 2,2-di-(3-methoxymethylphenyl)-1,3-propanediol (MMPPD) and cyclized NDGA (cNDGA) were isolated following literature procedures [14,23]. Citric acid, HCl and $MgSO_4$ were purchased from Fisher Scientific. All solvents, including formic acid were LC-MS grade. α-Synuclein (> 95% purity) was purchased from rPeptide (Watkinsville, GA, USA). Water was purified via a Millipore (Mississauga, ON) Milli-Q system with a Quantum EX Cartridge.

3.2 Instrumentation

3.2.1 HPLC-UV Diode Array Analysis

The autoxidation studies and reaction kinetics was performed on an Agilent 1200 high-performance liquid chromatography (HPLC) system (Agilent Technologies; Mississauga, ON) equipped with a degasser (G1379A), quaternary pump (G1311A), autosampler (G1329A), and diode array detector (G1315D). The HPLC column was a ThermoFisher Hypersil GOLD™ C_{18} (2.1 x 150 mm, 3µm), and the solvent system consisted of 0.1% LC-MS grade formic acid in water (solvent A) and 0.1% LC-MS grade formic acid in acetonitrile (solvent B) operating at a flow rate of 0.2 mL/min. Different methods were developed to ensure separation between the parent compounds and the oxidative metabolites. Method I: an initial isocratic condition at 90% solvent A for 5 minutes, decreased gradually to 60% solvent A over 5 minutes, then decreased to 10% over 15 minutes then returning to the initial conditions, with a 10 minute equilibration period prior to the next sample injection. Method II: an initial isocratic condition at 90% solvent A for 5

minutes, decreased gradually to 50% solvent A over 25 minutes, then 10% over 4 minutes then returning to the initial conditions, with a 7 minute equilibration period prior to the next sample injection. Method III: an initial isocratic condition at 90% solvent A for 2.5 minutes, decreased gradually to 10% solvent A over 22.5 minutes, then returning to the initial conditions, with a 10 minute equilibration period prior to the next sample injection. HPLC data was exported from OpenLab CDS ChemStation Edition C.01.09 (Santa Clara, California, USA) to GraphPad Prism version 8.0 for data analysis (San Diego, California, USA).

3.2.2 ESI-MS Analysis

Mass spectroscopy analysis of intermediates was conducted using an AB SCIEX 4000 QTRAP (Redwood City, CA, USA) quadrupole linear ion trap mass spectrometer. Final compounds were analyzed on an AB SCIEX QSTAR XL quadrupole orthogonal time-of-flight hybrid mass spectrometer (Q-TOF MS) equipped with an electrospray ionization (ESI) source (AB SCIEX, Redwood City, CA, USA). Samples were infused directly using a flow of 10 µL/min. Data acquisition and analyses were performed using Analyst 1.7 software from AB SCIEX.
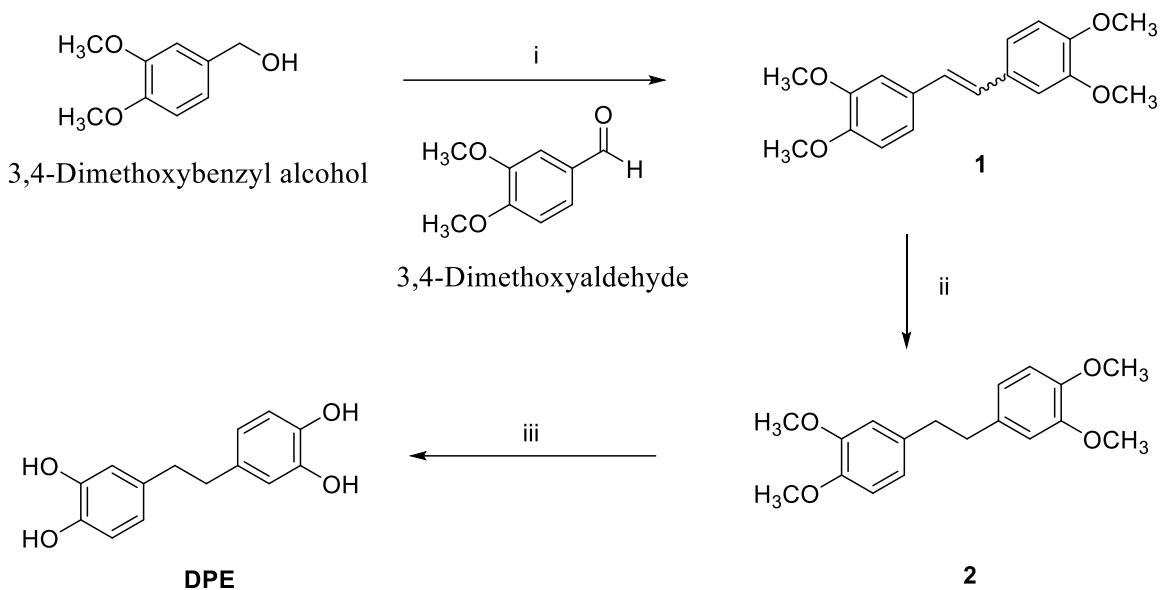
3.2.3 NMR Analysis

All NMR experiments were performed on a Bruker AVANCE DPX-500 spectrometer (Karlsruhe, Germany) and data processed using MestRreNova 14.1. All compounds were drawn and named using ChemDraw 20.0.

3.3 Methods

3.3.1 Synthesis and Characterization of Diphenyl Ethane Analogs

3.3.1.1 Synthesis of 4,4'-(ethane-1,2-diyl)bis(benzene-1,2-diol) (**DPE**)

Scheme 1. Synthesis of DPE. Reagents and Conditions: i) NBS, PPh$_3$, K$_2$CO$_3$, toluene, reflux, 37%; ii) H$_2$, Pd/C, THF, rt, >99%; iii) BBr$_3$/CH$_2$Cl$_2$, -78 °C, 88%.

Synthesis of 1,2-bis(3,4-dimethoxyphenyl)ethene (1): To a stirred solution of 3,4-dimethoxybenzyl alcohol (0.5 g, 2.97 mmol) and triphenylphosphine (1.87 g, 7.13 mmol) in toluene (15 mL), N-bromosuccinimide (0.29 g, 1.63 mmol) was added. The reaction mixture was refluxed under N$_2$ for 4 hours. After completion, the mixture was cooled to room temperature. At room temperature, 3,4-dimethoxyaldehyde (0.49 g, 2.97 mmol) was added followed by K$_2$CO$_3$ (4.1 g, 29.7 mmol) and then refluxed overnight. After cooling to room temperature, toluene was removed under reduced pressure. The residue was dissolved in ethyl acetate (EtOAc) and washed

with brine and dried over MgSO$_4$. After evaporation of solvents, the residue was recrystallized using isopropanol to give yield alkene (Z)-**1** as a white solid (0.4 g, 37%). ^{1}H NMR (500 MHz, CDCl$_3$) δ 7.06 (d, J = 2.0 Hz, 2H), 7.04 (dd, J = 8.2, 2.0 Hz, 2H), 6.93 (s, 2H), 6.86 (d, J = 8.2 Hz, 2H), 3.95 (s, 6H), 3.91 (s, 6H). ^{13}C NMR (126 MHz, CDCl$_3$) δ 149.25, 148.82, 130.80, 126.77, 119.70, 111.36, 108.68, 56.10, 56.00. ESI-MS (*m/z*) 323.1 [M + Na]$^+$.

Synthesis of 1,2-bis(3,4-dimethoxyphenyl)ethane (2): Pd/C (10% w/w, 40 mg) was added to a reaction flask under N$_2$. The flask was sealed, and dry tetrahydrofuran (THF) (10 mL) was added. The alkene **1** (400 mg, 1.33 mmol) in dry THF (2 mL) was added to the reaction dropwise. The flask was evacuated, then flushed with H$_2$ gas. The reaction was left to stir under H$_2$ overnight. The reaction mixture was filtered through a Celite pad and washed with methanol (MeOH). The solvent was removed under reduced pressure to give compound **2** as a white solid (0.4 g, 99%). ^{1}H NMR (500 MHz, CDCl$_3$) δ 6.79 (d, J = 8.1 Hz, 2H), 6.71 (dd, J = 8.0, 2.0 Hz, 2H), 6.66 (d, J = 2.0 Hz, 2H), 3.86 (s, 6H), 3.84 (s, 6H), 2.85 (s, 4H). ^{13}C NMR (126 MHz, CDCl$_3$) δ 148.66, 147.24, 134.55, 120.47, 112.02, 111.27, 56.07, 55.94, 37.88.

Synthesis of 4,4'-(ethane-1,2-diyl)bis(benzene-1,2-diol) (DPE): To a solution of **2** (0.4 g, 1.32 mmol) in dry CH$_2$Cl$_2$ (15 mL) at –78 °C under N$_2$, BBr$_3$ (5.3 mL, 5.28 mmol) was added dropwise. The reaction mixture was stirred and allowed to warm to room temperature overnight. After completion, the reaction mixture was poured onto crushed ice and extracted with EtOAc (3 × 15 mL). The organic layer was washed with water and brine and dried over Na$_2$SO$_4$ to give **DPE** as a purple solid (0.28 g, 88%). ^{1}H NMR (500 MHz, CD$_3$CN) δ 6.69 (d, J = 8.0 Hz, 2H), 6.64 (d, J =

2.0 Hz, 2H), 6.54 (dd, J = 8.0, 2.0 Hz, 2H), 6.50 (s, 2H), 6.44 (s, 2H), 2.70 (s, 4H). ^{13}C NMR (126 MHz, CD$_3$CN) δ 145.10, 143.28, 135.18, 120.96, 116.32, 115.88, 37.85. HRMS (TOF ESI-MS) calcd for $C_{14}H_{14}O_4$ (M+CH$_3$OH)$^+$ 279.0892, found 279.0953.

3.3.1.2 Synthesis of 2,3-Bis(3,4-dihydroxyphenyl)butane (**M2-DPE**)
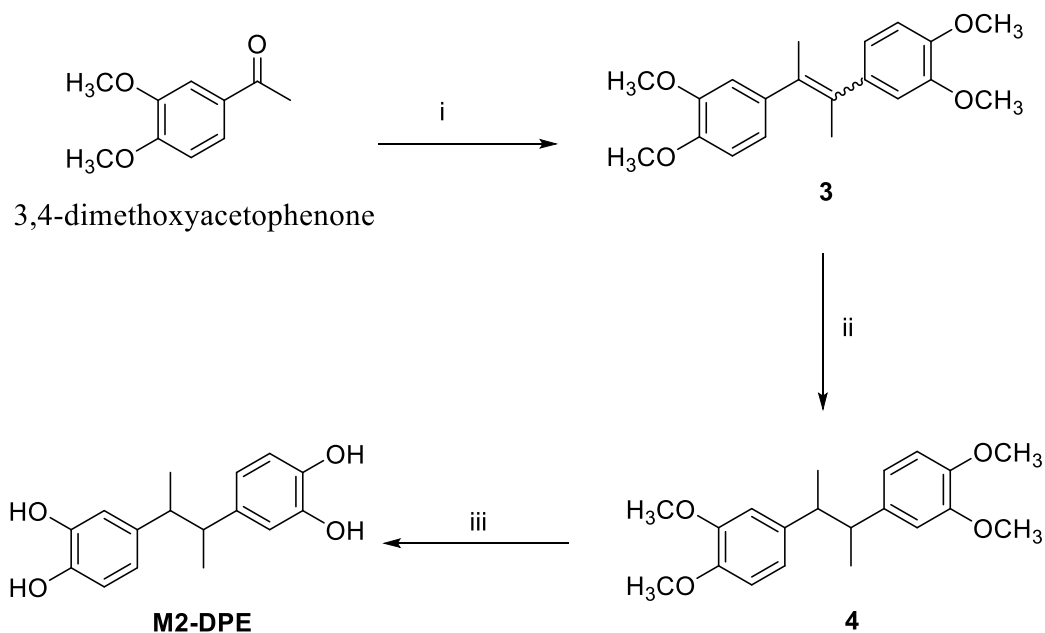
Scheme 2. Synthesis of M2-DPE. *Reagents and Conditions:* i) TiCl$_4$, Zinc, THF, -78 °C, 43%; ii) H$_2$, Pd/C, THF, rt, >99%; iii) BBr$_3$/CH$_2$Cl$_2$, -78 °C, 88%.

Synthesis of 4,4'-(but-2-ene-2,3-diyl)bis(1,2-dimethoxybenzene) (3): To a suspension of zinc powder (233.5 mg, 3.57 mmol) in dry THF (10 mL) at −78 °C under N$_2$, TiCl$_4$ (1.8 mL, 1.83 mmol) was added dropwise. Reaction was stirred at room temperature for 30 minutes and then refluxed. To this refluxing mixture, a solution of 3,4-dimethoxyacetophenone (100 mg, 0.55 mmol) in dry

THF (2 mL) was added, and the reaction mixture was refluxed overnight under N_2. After cooling to room temperature, the mixture was cooled to 0 °C. HCl 1M (30 mL) was added and then EtOAc (30 mL). After stirring at room temperature for 30 minutes, the mixture was filtered through a Celite pad. The aqueous layer was extracted with EtOAc (3 × 15 mL) and the organic layer was dried over Na_2SO_4. Solvent was evaporated, and the residue was purified by flash column chromatography (1:1 CH_2Cl_2/EtOAc) to afford **3** as a yellow oil (70 mg, 43%). ^{1}H NMR (500 MHz, CDCl₃) δ 6.65 (d, *J* = 8.3 Hz, 2H), 6.59 (dd, *J* = 8.2, 2.0 Hz, 2H), 6.46 (d, *J* = 2.0 Hz, 2H), 3.80 (s, 6H), 3.58 (s, 6H), 2.15 (s, 6H). ^{13}C NMR (126 MHz, CDCl₃) δ 148.77, 147.37, 121.13, 119.67, 111.08, 110.96, 56.03, 55.74, 47.06, 20.88. ESI-MS (*m/z*) 351.0 $[M + Na]^+$.

Synthesis of 4,4'-(butane-2,3-diyl)bis(1,2-dimethoxybenzene) (4): Pd/C (10% w/w, 7 mg) was added to a reaction flask under N_2. The flask was sealed, and dry THF (10 mL) was added. The alkene **3** (70 mg, 0.21 mmol) in dry THF (1 mL) was added to the reaction dropwise. The flask was evacuated, then flushed with H_2 gas. Reaction was left to stir under H_2 overnight. The reaction mixture was filtered through Celite pad and washed with MeOH (50 mL). The solvent was removed under pressure to give compound **4** as a white solid (66 mg, 60%). ^{1}H NMR (500 MHz, CDCl₃) δ 6.82 (d, *J* = 8.2 Hz, 2H), 6.74 (dd, *J* = 8.1, 2.0 Hz, 2H), 6.68 (d, *J* = 2.0 Hz, 2H), 3.88 (s, 6H), 3.87 (s, 6H), 2.75 – 2.70 (m, 2H), 1.04 (d, *J* = 6.6 Hz, 6H). ^{13}C NMR (126 MHz, CDCl₃) δ 148.79, 147.37, 139.14, 119.67, 111.08, 110.96, 56.03, 55.99, 47.07, 20.89. ESI-MS (*m/z*) 353.2 $[M + Na]^+$.

Synthesis of 4,4'-(butane-2,3-diyl)bis(benzene-1,2-diol) (M2-DPE): To a solution of **4** (66 mg,

0.19 mmol) in dry CH_2Cl_2 (5 mL) at −78 °C under N_2, BBr_3 (0.8 mL, 0.79 mmol) was added dropwise. The reaction mixture was stirred and allowed to warm to room temperature overnight. After completion, reaction mixture was poured onto crushed ice and extracted with EtOAc (3 × 15 mL). The organic layer was washed with water (15 mL) and brine (15 mL) and dried over $MgSO_4$ to give **M2-DPE** as a purple solid (11 mg, 20%). ^{1}H NMR (500 MHz, CD_3CN) δ 6.74 (d, $J = 8.1$ Hz, 2H), 6.70 (d, $J = 2.0$ Hz, 2H), 6.60 (dd, $J = 8.1, 2.1$ Hz, 2H), 6.49 (s, 2H), 6.47 (s, 2H), 2.62 – 2.57 (m, 2H), 0.91 (d, $J = 6.5$ Hz, 6H).^{13}C NMR (126 MHz, CD_3CN) δ 145.18, 143.31, 140.11, 120.09, 115.86, 115.23, 47.20, 21.51. HRMS (TOF ESI-MS) calcd for $C_{16}H_{18}O_4$ (M-H)[-] 273.1205, found 273.1130.

3.3.1.3 Synthesis of 4,4'-(2,3-dimethylbutane-2,3-diyl)bis(benzene-1,2-diol) (**M4-DPE**)
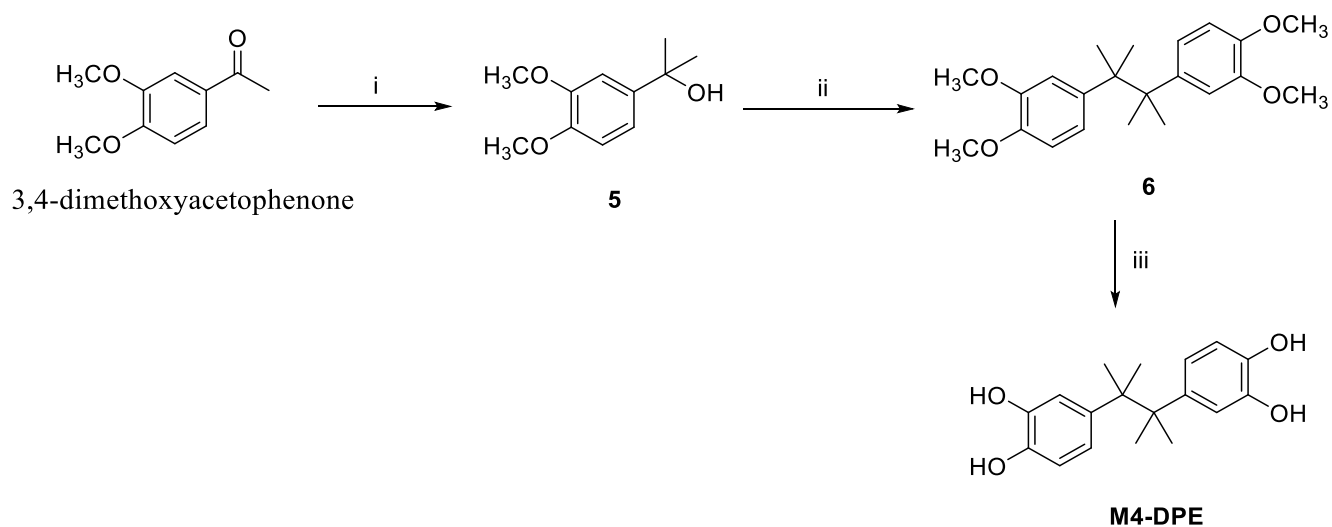
Scheme 3. Synthesis of M4-DPE. *Reagents and Conditions:* i) $MgCH_3I$, Et_2O, rt, 41%; ii) $TiCl_4$, Zinc, THF, -78 °C, 20%; iii) BBr_3/CH_2Cl_2, -78 °C, 91%

Synthesis of 2-(3,4-dimethoxyphenyl)propan-2-ol (5): Magnesium turnings (31 mg, 1.27 mmol) were added to an oven-dried flask with 5 mL of ether. Iodomethane (181 mg, 1.27 mmol) was dissolved in ether (3 mL) and added dropwise to the reaction. Magnesium turnings were crushed with a glass rod, and the reaction initiated. After completion, the reaction mixture was cooled to 0 °C and 3,4-dimethoxyacetophenone (91 mg, 0.5 mmol) were added dropwise under N_2. After stirring overnight, the reaction mixture was cooled 0 °C and 2M HCl (2 mL) was added dropwise, and the mixture extracted with EtOAc (3 × 15 mL). The organic layer was dried over $MgSO_4$, and solvent evaporated. The residue was purified by flash column chromatography (2:1 hexane/EtOAc) to afford **5** as a yellow oil (40 mg, 41%). ^{1}H NMR (500 MHz, $CDCl_3$) δ 7.09 (d, $J = 2.2$ Hz, 1H), 6.98 (dd, $J = 8.3, 2.2$ Hz, 1H), 6.83 (d, $J = 8.4$ Hz, 1H), 3.91 (s, 4H), 3.88 (s, 3H), 1.58 (s, 6H). ^{13}C NMR (126 MHz, $CDCl_3$) δ 148.77, 147.85, 142.06, 116.46, 110.75, 108.34, 72.51, 56.05, 56.01, 31.94. ESI-MS (*m/z*) 219.1 [M + Na]$^+$.

Synthesis of 4,4'-(2,3-dimethylbutane-2,3-diyl)bis(1,2-dimethoxybenzene) (6): To a suspension of zinc powder (87.6 mg, 1.34 mmol) in dry THF (10 mL) at –78 °C under N_2, $TiCl_4$ (0.7 mL, 0.68 mmol) was added dropwise. The reaction was stirred at room temperature for 30 minutes and then refluxed. To this refluxing mixture, a solution of the tertiary alcohol **5** (40 mg, 0.2 mmol) in dry THF (1 mL) was added, and the reaction mixture was refluxed overnight under N_2. After cooling to room temperature, the mixture was cooled to 0 °C. HCl 1M (10 mL) was added and then EtOAc (15 mL). After stirring at room temperature for 30 minutes, the mixture was filtered through a Celite pad. The aqueous layer was extracted with EtOAc (3 × 15 mL) and

the organic layer was dried over MgSO$_4$. The solvent was evaporated, and the residue was purified by flash column chromatography (4:1 hexane/EtOAc) to afford **6** as a yellow oil (17 mg, 20 %). ^{1}H NMR (500 MHz, CDCl$_3$) δ 6.71 (d, J = 8.5 Hz, 1H), 6.64 (dd, J = 8.4, 2.2 Hz, 1H), 6.39 (d, J = 2.2 Hz, 1H), 3.85 (s, 3H), 3.66 (s, 3H), 1.32 (s, 6H). ^{13}C NMR (126 MHz, CDCl$_3$) δ 146.97, 146.96, 139.73, 121.04, 113.04, 109.42, 55.93, 55.75, 43.71, 25.42. ESI-MS (*m/z*) 381.2 [M + Na]$^+$.

Synthesis of 4,4'-(2,3-dimethylbutane-2,3-diyl)bis(benzene-1,2-diol) (M4-DPE): To a solution of **6** (17 mg, 0.04 mmol) in dry CH$_2$Cl$_2$ (5 mL) at –78 °C under N$_2$, BBr$_3$ (0.2 mL, 0.19 mmol) was added dropwise. The reaction mixture was stirred and allowed to warm to room temperature overnight. After completion, the reaction mixture was poured onto crushed ice and extracted with EtOAc (3 × 15 mL). The organic layer was washed with water (15 mL) and brine (15 mL) and dried over MgSO$_4$ to give **M4-DPE** as a purple solid (13 mg, 91 %). ^{1}H NMR (500 MHz, CD$_3$CN) δ 6.62 (d, J = 8.3 Hz, 2H), 6.53 (d, J = 2.3 Hz, 2H), 6.49 (dd, J = 8.4, 2.4 Hz, 2H), 1.20 (s, 12H). ^{13}C NMR (126 MHz, CD$_3$CN) δ 143.46, 142.93, 140.26, 121.37, 117.14, 114.13, 43.74, 25.88. HRMS (TOF ESI-MS) calcd for C$_{18}$H$_{22}$O$_4$ (M-H)$^-$ 301.1518, found 301.1438.

3.3.1.4 Synthesis of 2,3,6,7-tetrahydroxy-9,10-dihydrophenanthrene (**o-DPE B**)
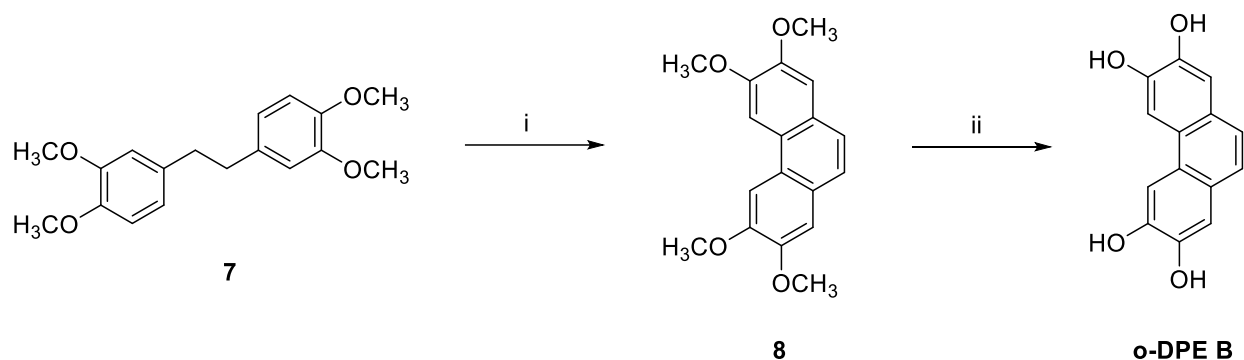
Scheme 4. Synthesis of o-DPE B. *Reagents and Conditions:* i) BF$_3$·OEt$_2$, PIFA, CH$_2$Cl$_2$, -20 °C, 11%; ii) BBr$_3$/ CH$_2$Cl$_2$, -78 °C, 92%

Synthesis of 2,3,6,7-tetramethoxyphenanthrene (8): First, a solution of bis(trifluoroacetoxy)iodobenzene (PIFA) (365.5 mg, 0.85 mmol) and BF$_3$·OEt$_2$ (0.16 mL, 1.3 mmol) in CH$_2$Cl$_2$ (2 mL) was prepared and cooled at -20 °C. This solution was added dropwise over 15 minutes to a solution of **7** (172.3 mg, 0.57 mmol) in CH$_2$Cl$_2$ (5 mL) at -20 °C under nitrogen. The solution was stirred at -20 °C for 40 minutes. After completion, the solvent was removed under pressure, and the residue purified by flash column chromatography (1:2 EtOAc/hexane) to afford **8** as a yellow solid (86 mg, 51 %). ^{1}H NMR (500 MHz, CDCl3) δ 7.81 (s, 1H), 7.56 (s, 1H), 7.23 (s, 1H), 4.13 (s, 3H), 4.04 (s, 3H).

Synthesis of phenanthrene-2,3,6,7-tetraol (o-DPE B): To a solution of **8** (20 mg, 0.067 mmol) in dry CH$_2$Cl$_2$ (2 mL) at –78 °C under N$_2$, BBr$_3$ (0.26 mL, 0.268 mmol) was added dropwise. The reaction mixture was stirred and allowed to warm to room temperature overnight. After completion, reaction mixture was poured onto crushed ice and extracted with EtOAc (3 × 15 mL).

The organic layer was washed with water (15 mL) and brine (15 mL) and dried over MgSO$_4$ to give **o-DPE B** as a brown solid (15 mg, 92%). ^{1}H NMR (500 MHz, MeOD) δ 7.77 (s, 1H), 7.29 (s, 1H), 7.11 (s, 1H). ^{13}C NMR (126 MHz, MeOD) δ 147.06, 146.26, 127.41, 125.75, 124.29, 112.73, 107.40. ESI-MS (*m/z*) 241.02 [M - H]$^-$.

3.3.2 Chemical Stability and Reaction Kinetics

Test compounds in CH$_3$CN (20 mM) were incubated in phosphate-citric acid buffer (0.5 M, pH 7.4) at 37 °C to yield a final concentrations of 0.5 mM each [24]. Before adding the compound, buffer was treated under three conditions: nitrogen purged, oxygen purged or ambient conditions (no purging). The mixture was then incubated at 37 ºC using an Orbital Shaker (VWR). Aliquots (90 µL) were taken at different times and quenched by adding 2M HCl (30 µL) spiked with internal standard 2,2-di-(3-methoxymethylphenyl)-1,3-propanediol (MMPPD). The samples were analyzed directly by HPLC-UV. The kinetics of the loss of the diphenylethanes were established from the concentration that remained in the buffer solution over time [24]. The loss of diphenylethanes in buffer at pH 7.4 follows apparent first-order kinetics. Therefore, the rate of loss can be described by:

$$ln\frac{C}{C_o} = -k_{dep} \tag{3.1}$$

Where C_0 and C are initial concentration and concentration at time *t* respectively; k_{dep} is the reaction rate for loss of starting material and *t* is time. k_{dep} was obtained as the gradient from a plot of ln $(\frac{C}{C_o})$ as a function of time t.

3.3.3 Quantification of DPEs and autoxidation products

Standard curves were prepared in triplicates for the DPEs (DPE, M2-DPE, and M4-DPE) ranging from 10 to 500 µM at a wavelength of 280 nm, and for o-DPE B ranging from 10 to 100 µM at a wavelength of 254 nm. Calibration curves were calculated by using linear regression analysis using GraphPad Prism version 8.0 (San Diego, California, USA).

3.3.4 Thioflavin T Assay

The protein α-synuclein (AS) was diluted in phosphate buffered saline (PBS) at a concentration of 2 mg/mL. Experiments were performed in triplicate with or without test compounds at final concentrations of 100 and 500 µM in PBS at pH 7.4. Both drug and protein were added to a microcentrifuge tube producing 1.5 mg/mL of AS. The mixture was incubated for 5 days at 37 °C shaking at 1400 rpm using a Thermomixer R (Eppendorf, Hamburg, Germany). Upon completion, 10 µL of each mixture was pipetted in triplicate onto a 96-well plate containing 144 µL of Thioflavin-T (ThT) solution (26 µM) and fluorescence was measured with a Molecular Devices SpectraMax M2 microplate reader (San Jose, USA) at excitation of 444 nm and emission of 484 nm. Data analysis was performed by averaging the readings per tube and comparing with control and/or different concentrations using one-way ANOVA.

4　Results

4.2 Synthesis and characterization of diphenylethane analogs

　　We prepared three diphenylethane analogs (DPE, M2-DPE, M4-DPE, Figure 2), all three were prepared through coupling reactions involving 3,4-dimethoxyphenyl derivatives.
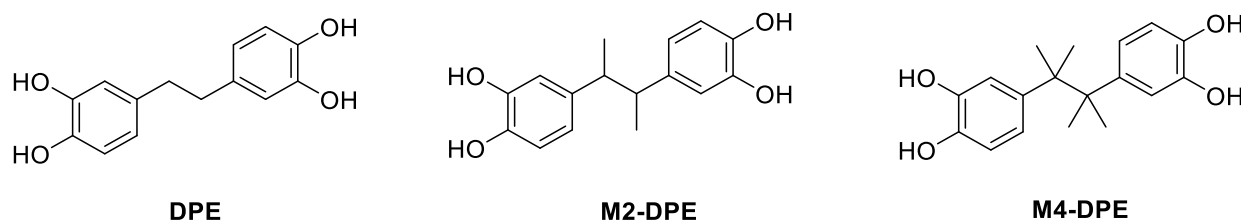
Figure 2. Proposed diphenylethanes with 0 (DPE), 2 (M2-DPE), and 4 (M4-DPE) methyl groups on the side chain.

　　The diphenylethane derivative with no substituents on the alkyl linker chain, 4, 4'-(ethane-1,2-diyl)bis(benzene-1,2-diol) (DPE), was prepared using a literature procedure for the preparation of the tetramethoxy precursor (Scheme 1) [21]. We employed a Wittig reaction between 3,4-dimethoxybenzyl alcohol and 3,4-dimethoxybenzaldehyde in the first step to yield the tetramethoxy alkene intermediate as a white solid in 37% yield. The alkene was hydrogenated over Pd/C under H_2 atmosphere to give the corresponding saturated compound in 99% yield. We obtained the final compound, DPE, through boron tribromide demethylation of the tetramethoxy alkane intermediate in DCM at -78 °C in 88% yield for a 32% overall yield. We confirmed that we had DPE through high-resolution time-of-flight electrospray mass spectrometry (negative mode) which yielded an *m/z* of 279.0953. In our ^{1}H NMR we observed aromatic C-H signals at δ6.69, 6.64 and 6.54, aromatic OH signals at δ6.50 and 6.44 and a benzyl H signal at δ2.70. Due to the symmetry of DPE, the benzyl protons appear as a singlet corresponding to 4H.

We prepared 2,3-bis(3,4-dihydroxyphenyl)butane (M2-DPE) by first carrying out a McMurray coupling using Zn and $TiCl_4$ to combine 2 molecules of 3,4-dimethoxyacetophenone to produce the alkene intermediate in 43 % yield (Scheme 2) [25]. We isolated the *Z*-isomer based on comparison with the literature coupling constants, but we observed a negligible amount of *E*-isomer and therefore did not collect it. We subsequently reduced the alkene to a mixture of alkane isomers (meso and racemic) via hydrogenation over Pd/C in 60% yield and the methoxy groups were removed with boron tribromide to give M2-DPE (20% yield) to give 23% overall yield. We confirmed the structure of M2-DPE through high-resolution time-of-flight electrospray mass spectrometry (negative mode) which gave an *m/z* of 273.1130. We further confirmed the structure from observed NMR signals at δ6.74, 6.70, 6.60 (Aromatic C-H), δ6.49, 6.47 (Aromatic OH), δ2.57-2.62 (benzyl H) and δ0.91 (CH_3). Unlike DPE, the benzyl protons of M2-DPE appear as a multiplet from δ2.57-2.62 due to coupling with the adjacent methyl protons (δ0.91) and the mixture of meso and racemic isomers.

The starting material needed for M4-DPE, 2-(3,4-dimethoxyphenyl)propan-2-ol, was prepared via methyl magnesium iodide methylation of 3,4-dimethoxyacetophenone in 41% yield (Scheme 5) [26]. We then coupled two 2-(3,4-dimethoxyphenyl)propan-2-ol units by treatment with Zn and $TiCl_4$ at -78 °C in dry THF to produce the tetramethoxy alkane linked product (20% yield). The di-catechol was realized via boron tribromide deprotection of the methoxy groups (91% yield) for an overall yield of 7%. We confirmed the structure of M4-DPE through high-resolution time-of-flight electrospray mass spectrometry (negative mode) which gave an *m/z* of 301.1438. Similar to DPE, M4-DPE is symmetrical so that the methyl groups appear as a singlet of 12H at δ1.20.

DPE and M4-DPE exist as single entities however M2-DPE is likely present as a mixture

of the meso compound and a racemic mixture; we could not separate the isomers so the isomeric mixture was used as is for the autoxidation experiments.

4.3 Autoxidation of diphenylethane analogs

4.3.1   Rates of autoxidation of diphenylethanes at pH 7.4

The three di-catechol diphenylethanes, DPE, M2-DPE, and M4-DPE, were investigated for their ability to autoxidize to their corresponding dibenzocyclohexadienes. The spontaneous cyclization in buffer was carried out using a protocol already established in our group [24]. DPE, M2-DPE, or M4-DPE and internal standard (MMPPD) were incubated in phosphate-citric acid buffer (0.5 M, pH 7.4) at 37 °C to a final concentration of 0.5 mM each. Aliquots were taken at different times for DPE, M2-DPE, and M4-DPE (Table S1). The reaction was stopped by acidifying to pH 1.5 with HCl. Samples were analyzed by HPLC using Method I (DPE and M4-DPE) or Method II (M2-DPE) (Table S2). Each compound was investigated under three conditions: (i) N_2 purged, (ii) O_2 purged and (iii) ambient conditions to confirm that loss of starting material was an autoxidative process.

The autoxidation kinetics were determined by following the loss of starting compound in phosphate-citric acid buffer over time, which was calculated using peak area ratio of starting compound and internal standard. The rate of loss (k_{dep}) of DPE, M2-DPE and M4-DPE followed pseudo first-order kinetics. Figure 3 shows the results for the loss of starting di-catechol diphenylethane against time.
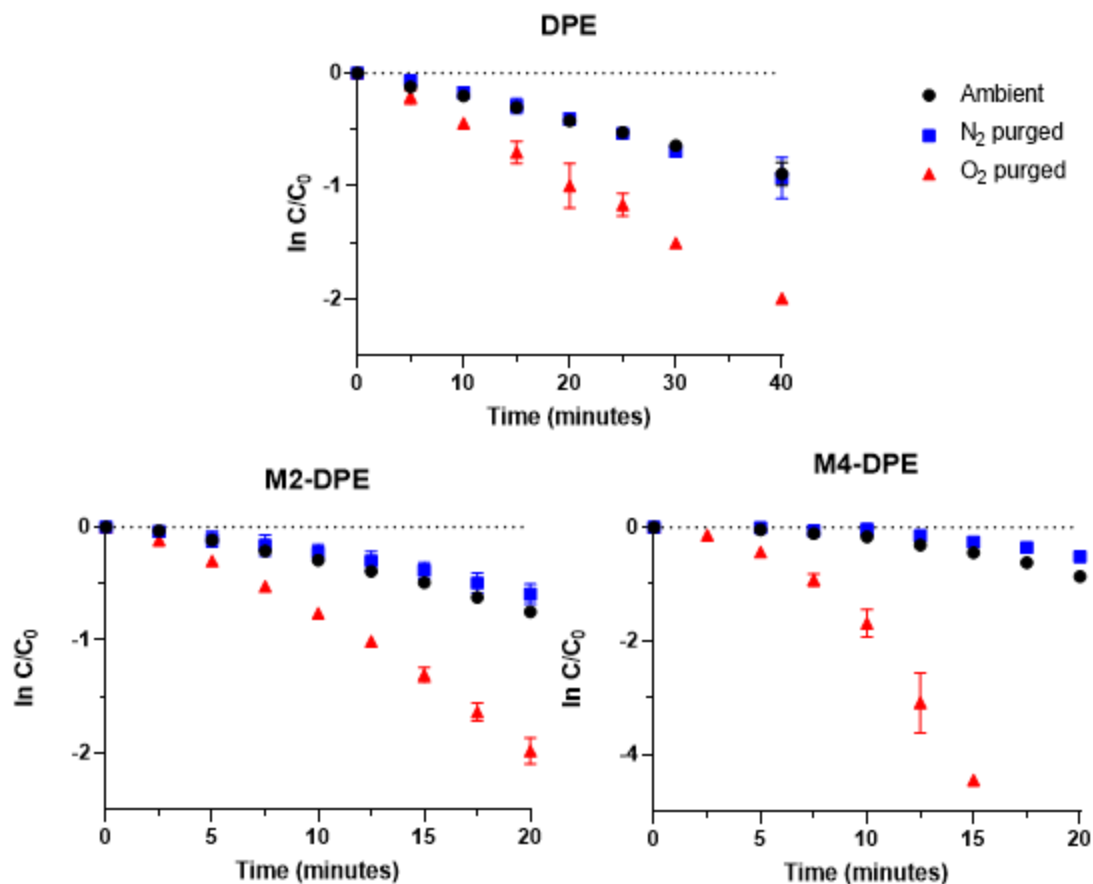
Figure 3. Plot of ln C/C_0 *vs* time of DPE (n=3), M2-DPE (n=3), and M4-DPE (n=3) in phosphate-citric buffer (pH 7.4) at 37 °C using different experimental conditions.

For all three compounds, the loss of diphenylethane starting material occurs most rapidly for the O_2 purged sample; the rate of loss for the N_2 purged samples was the slowest although the difference compared to the ambient conditions is small (Table 1). The ratio of the O_2 purged versus the N_2 purged rates ($k_{dep}(O_2)/k_{dep}(N_2)$) is: 1.55 (DPE); 2.33 (M2-DPE); 4.48 (M4-DPE). Our data show that the rate of loss is dependent on the number of methyl groups on the alkyl linker as the rate of decomposition increases with the number of methyl groups for all three experimental conditions.

Table 1. Autoxidation rate of DPE (n=3), M2-DPE (n=3), and M4-DPE (n=3) in phosphate-citric acid buffer (pH 7.4) at 37 °C using different experimental conditions.

| Compound	Ambient		Nitrogen		Oxygen	
	k_{dep} (min^{-1})	$t_{1/2}$ (min)	k_{dep} (min^{-1})	$t_{1/2}$ (min)	k_{dep} (min^{-1})	$t_{1/2}$ (min)
DPE	$2.87 \times 10^{-2} \pm 0.0006$	24.14	$2.84 \times 10^{-2} \pm 0.0012$	24.4	$4.4 \times 10^{-2} \pm 0.0011$	15.75
M2-DPE	$6.16 \times 10^{-2} \pm 0.0016$	11.25	$4.93 \times 10^{-2} \pm 0.0033$	14.05	$1.15 \times 10^{-1} \pm 0.0057$	6.02
M4-DPE	$9.0 \times 10^{-2} \pm 0.012$	7.7	$6.53 \times 10^{-2} \pm 0.0061$	10.61	$2.93 \times 10^{-1} \pm 0.0173$	2.36

4.3.2 Products of diphenylethane autoxidation at pH 7.4

We hypothesized that the di-catechol diphenylethane derivatives would undergo intramolecular cyclization to dibenzocyclohexadienes at pH 7.4. We determined that for DPE three distinct products resulted from autoxidation (Figure 4), whereas two distinct products were formed for each of M2-DPE (Figure 5) and M4-DPE (Figure 6).
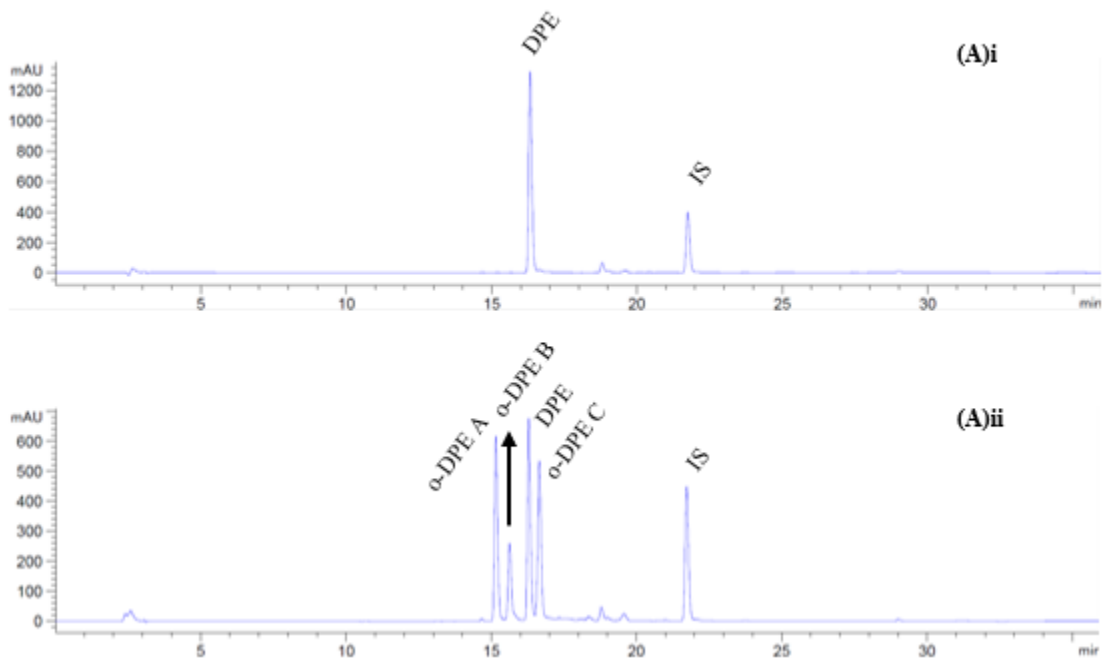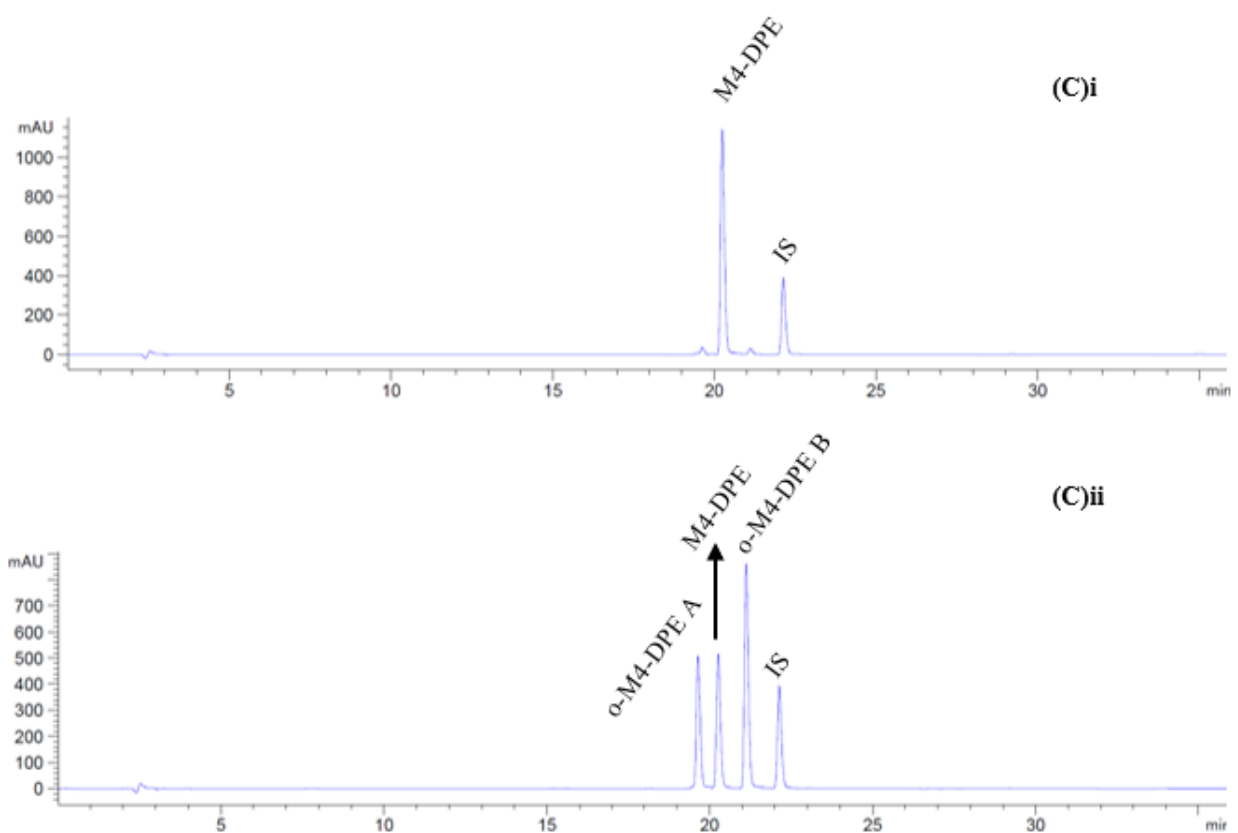

Figure 4. HPLC chromatogram for DPE incubation (pH 7.4) at 37 ℃ at time 0 (i) and 20 minutes (ii). DPE retention time was observed at 16.3 minutes, while for its oxidized products were 15.1 minutes (o-DPE A), 15.6 minutes (o-DPE B), and 16.6 minutes (o-DPE C). IS is the internal standard (MMPPD) at 21.7 minutes.
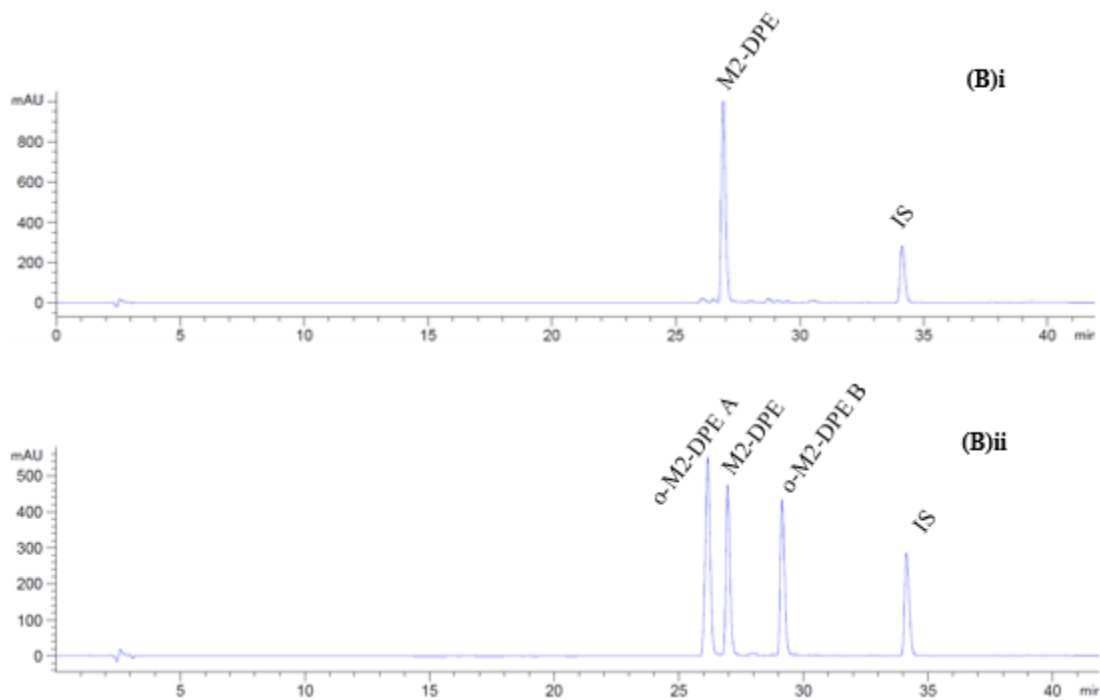
Figure 5. HPLC chromatogram for M2-DPE incubation (pH 7.4) at 37 ℃ at time 0 (i) and 10 minutes (ii). M2-DPE retention time was observed at 26.9 minutes, while for its oxidized products were 26.1 minutes (o-M2-DPE A) and 29.1 minutes (o-M2-DPE B). IS is the internal standard (MMPPD) at 34.1 minutes.

Figure 6. HPLC chromatogram for M4-DPE incubation (pH 7.4) at 37 ℃ at time 0 (i) and 7.5 minutes (ii). M4-DPE retention time was observed at 20.2 minutes, while for its oxidized products were 19.6 minutes (o-M4-DPE A) and 21.1 minutes (o-M4-DPE B). IS is the internal standard (MMPPD) at 22.1 minutes.

For our di-catechol diphenylethanes, we isolated the product peaks through reverse-phase preparative chromatography and analyzed the isolated products via HPLC, NMR and mass spectrometry. Several of the decomposition products displayed poor solubility in typical NMR solvents (chloroform, acetonitrile, methanol, DMSO) so we used a mixed solvent system consisting of D_2O, CD_3CN and DCl. All of our compounds were soluble in this mixed system allowing us to compare NMR spectra across the DPE derivatives and their autoxidation products. Since the compounds were stable in an acidic environment (HCl was used to quench the

autoxidation reaction) we observed no stability issues with the D_2O/ CD_3CN/ DCl solvent system. However, products o-M2-DPE A and o-M4-DPE A still displayed limited solubility in the solvent system, and due to the low concentration we were unable to generate satisfactory ^{13}C NMR.

4.3.2.1 Autoxidation products of **DPE**

DPE formed three autoxidation products (Figure 7), two were formed directly from DPE (o-DPE A and o-DPE C). When we subsequently exposed isolated o-DPE A and o-DPE C to our autoxidation conditions we observed that o-DPE A formed o-DPE B, whereas o-DPE C formed an additional product which was trapped as a GSH adduct (see section 4.3.4). o-DPE A had an ESI (-) *m/z* 242.9 corresponding to a MW of 244, and the ^{1}H NMR showed aromatic singlets at $\delta6.60$ and $\delta7.02$ each representing one proton and a singlet at $\delta2.61$ of four protons. This was consistent with intramolecular cyclization to form the dibenzocyclohexadiene 2,3,6,7-tetrahydroxy-9,10-dihydrophenanthrene. o-DPE B had an ESI (-) *m/z* of 241.02 corresponding to a MW of 242 and a ^{1}H NMR showing three aromatic singlets at $\delta7.11$, $\delta7.29$ and $\delta7.77$ consistent with aromatization of the cyclohexadiene ring to form 2,3,6,7-tetrahydroxy-phenanthrene. This was confirmed through formation of the phenanthrene using the method of Zeng & Chemler (2008) [27] which was identical to o-DPE B (Scheme 4).
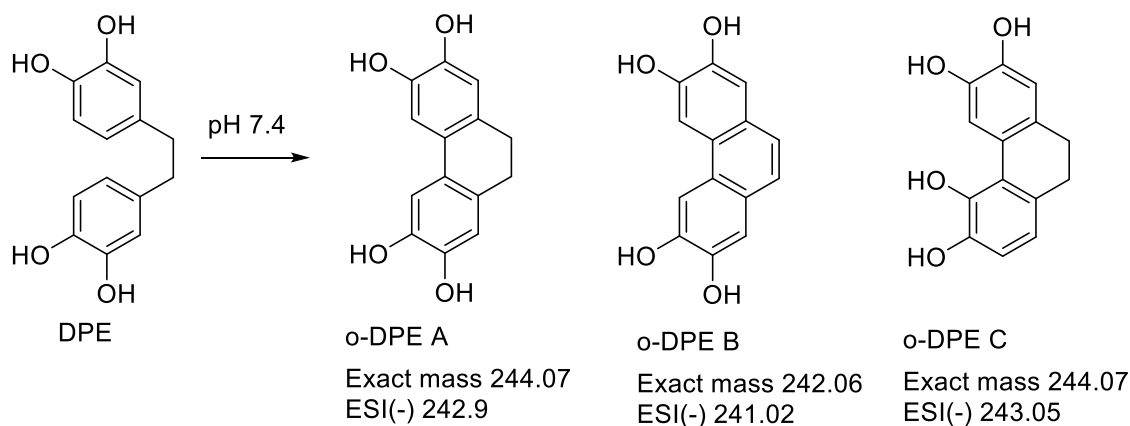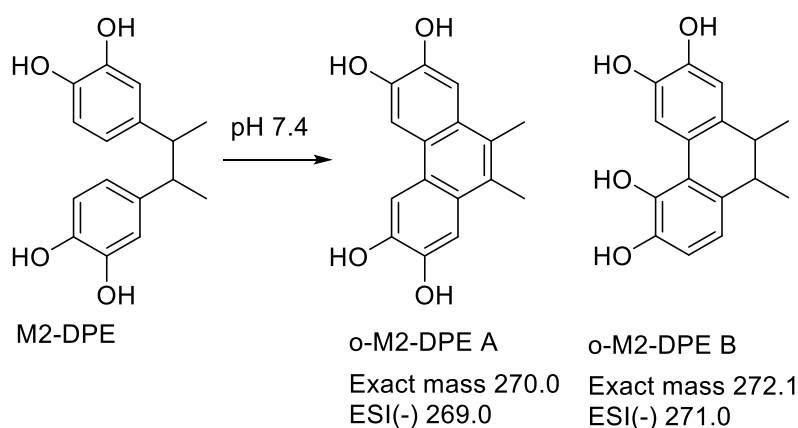
Figure 7. DPE and its oxidized products formed in phosphate buffer (pH 7.4) at 37 ºC. Exact mass and *m/z* (ESI negative ion mode) are shown for each product.

Finally, we investigated o-DPE C which was formed directly from DPE. We determined that o-DPE C had an ESI (-) *m/z* of 243.05 corresponding to a MW of 244 and ^{1}H NMR that in the aromatic region showed a pair of doublets at δ7.15 and δ7.21 of one proton each and singlets at δ7.25 and δ8.44 of one proton each and a multiplet at δ3.13 of four protons corresponding to the CH$_2$ protons. This suggested to us that intramolecular cyclization had occurred, but that substitution had occurred at different positions on the aromatic rings. Our HSQC and COSY results supported this observation leading us to conclude that o-DPE C is 2,3,5,6-tetrahydroxy-9,10-dihydrophenanthrene. Unlike o-DPE A, we did not observe formation of a corresponding aromatized product derived from o-DPE C.

4.3.2.2 Autoxidation products of M2-DPE

The two HPLC peaks observed for the M2-DPE autoxidation elute at 26.1 min (o-M2-DPE A) and 29.1 min (o-M2-DPE B), whereas M2-DPE elutes at 26.9 min. For o-M2-DPE A we observed an ESI (-) *m/z* 269.0 corresponding to a MW of 270 and for o-M2-DPE B we observed

an ESI (-) *m/z* 271.07, corresponding to a MW of 272. For o-M2-DPE A we observed that the [1]H

NMR was similar to o-DPE B as there were three aromatic singlets (δ7.38, 7.79, and 8.12) each

integrating to one proton and a singlet at δ2.49 integrating to three protons. Together these results

in addition to the lack of C-H signals suggested to us the o-M2-DPE A is 2,3,6,7-tetrahydroxy-

9,10-dimethylphenanthrene. In contrast, we observed that o-M2-DPE B displayed ^{1}H NMR

characteristics similar to o-DPE C with doublets at δ6.57 and δ6.67 integrating to one proton each

and singlets at δ6.68 and δ7.85 or 8.25 integrating to one proton each. In addition, multiplets at

δ1.2-1.29 (3H), δ2.61-2.65 (1H) and δ2.7-2.73 (3H) correspond to CH$_3$ and CH. From this data

we concluded that o-M2-DPE B is 2,3,5,6-tetrahydroxy-9,10-dimethylphenanthrene (Figure 8).

Figure 8. M2-DPE and its oxidized products formed in phosphate buffer (pH 7.4) at 37 °C. Exact

mass and *m/z* (ESI negative ion mode) are shown for each product.

These results are consistent with intramolecular cyclization and formation of a new C-C

bond between the aromatic rings. Our ^{1}H NMR analysis was complicated by the potential presence

of both meso and racemic M2-DPE starting material. In the cyclized products loss of free rotation

of the alkyl linker may be anticipated to result in different chemical shifts and coupling constants

for meso and racemic o-M2-DPEs. The methyl groups of the meso o-M2-DPE B would be in axial/

equatorial positions leading to the benzyl protons adopting dihedral torsion angles of approximately 45°; the racemic o-M2-DPE B would likely place the methyl groups in a di-axial position with the dihedral torsion angles of the benzyl protons closer to 60°. From the Karplus equation we would anticipate a coupling constant for the benzyl protons of approximately 6-10 Hz for the potential products. In the chemical shift range 2.6-2.7 we can observe overlapping doublets of quartets, but we were unable to calculate the coupling constant due to the presence of the mixture of diastereomers.

4.3.2.3 Autoxidation products of M4-DPE

Since the alkyl linker of M4-DPE already possesses adjacent dimethyl substituted carbons we anticipate that a fully aromatized cyclic product analogous to o-DPE B and o-M2-DPE A could not be formed. We observed two HPLC peaks for M4-DPE autoxidation that elute at 19.6 min (o-M4-DPE A) and 21.1 min (o-M4-DPE B), whereas M4-DPE elutes at 20.2 min. For o-M4-DPE A we observed an ESI (-) *m/z* 299.08 (MW 300) and for o-M4-DPE B we observed an ESI (-) *m/z* 299.1 (MW 300). This suggested that both autoxidation products are consistent with intramolecular cyclization and formation of a new C-C bond between the aromatic rings. Our ^{1}H NMR for o-M4-DPE A displayed aromatic singlets at δ6.82 (1H) and δ7.03 (1H) and singlets at δ3.23 (3H) and δ8.12 (1H). For o-M4-DPE B the ^{1}H NMR displayed doublets at δ6.67 (1H) and δ6.73 (1H) and a singlet at δ6.83 (1H) in the aromatic region, and singlets at δ7.87 (1H) and δ8.12 (1H). We observed singlets at δ0.72, δ0.76, δ1.29 and δ1.30 each integrating to three protons that correspond to the four CH_3 groups. Together these results suggested to us that o-M4-DPE A is 2,3,6,7-tetrahydroxy-9,9,10,10-tetramethylphenanthrene and o-M4-DPE B is 2,3,5,6-tetrahydroxy-9,9,10,10-tetramethylphenanthrene (Figure 9).
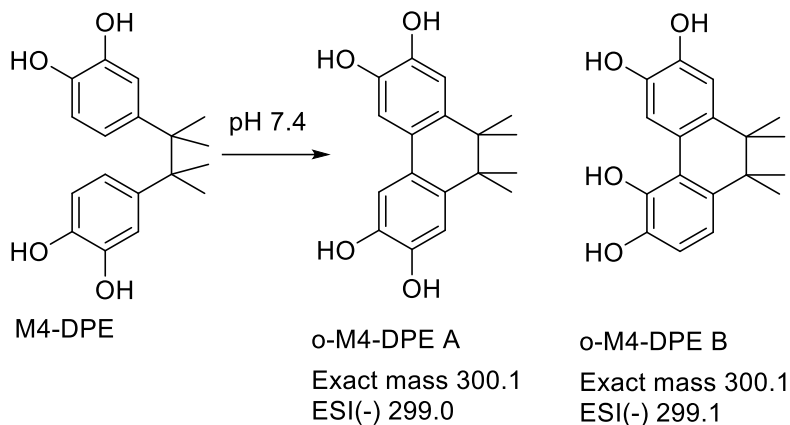
Figure 9. M4-DPE and its oxidized products formed in phosphate buffer (pH 7.4) at 37 °C. Exact mass and *m/z* (ESI negative ion mode) are shown for each product.

We compared the HPLC-UV absorption spectra of our diphenylethane autoxidation products and observed that the spectra for o-DPE A and o-M4-DPE A are similar in appearance (λ 276, 328 nm and λ 280, 325 nm respectively) corresponding to the 2,3,6,7-tetrahydroxy phenanthrene structure, whereas the spectra for o-DPE C, o-M2-DPE B, and o-M4-DPE B are also similar in appearance (λ 279, 304 nm, λ 280, 304 nm and λ 280, 306 nm respectively) corresponding to the 2,3,5,6-tetrahydroxy phenanthrene structure. Finally, the UV spectra for o-DPE B and o-M2-DPE A are similar in appearance (λ 254, 289, 305 nm and λ 256, 291, 308 nm respectively) corresponding to the aromatized 2,3,6,7-tetrahydroxy phenanthrene structure (Figure 10).
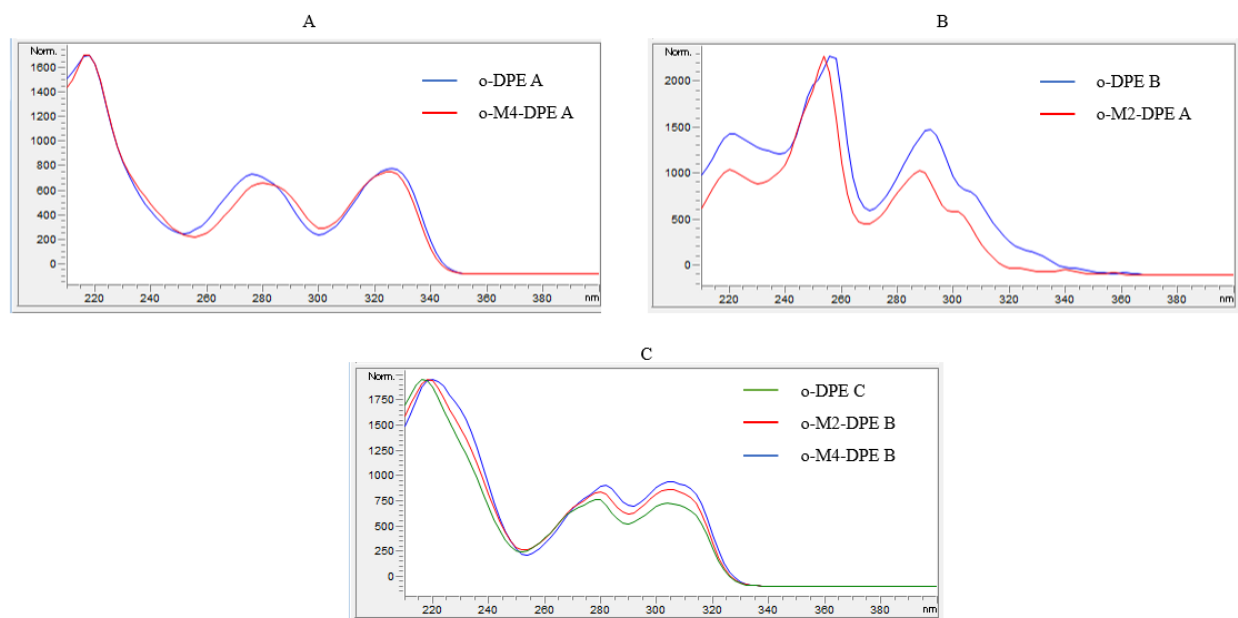
Figure 10. UV absorption extracted from HPLC chromatogram for all the oxidized products grouped in three panels (A, B, C) according to their structure similarity. Panel A contains cyclized symmetrical o-DPE A and o-M4-DPE A; Panel B contains cyclized fully aromatized o-DPE B and o-M2-DPE A; Panel C contains asymmetrical cyclized o-DPE C, o-M2-DPE B, and o-M4-DPE B.

4.3.3 Quantification of DPEs and autoxidation products in the incubation mixture

The concentration of each DPE and their autoxidation products were determined from the standard curves prepared (Figure S13). We extrapolated the standard curves from each DPE to their respective autoxidative metabolite with the exception of o-DPE B and o-M2-DPE A. We prepared a standard curve for o-DPE B at 254 nm, and extrapolated to o-M2-DPE A given the same UV absorption profile. We observed that for both DPE and M2-DPE symmetric cyclization predominated, whereas for M4-DPE asymmetric cyclization was greater.

Table 2. Concentration of DPEs and their autoxidative products at 10 minutes of incubation

Compound	Concentration (µM)	%
DPE	220.8	44
o-DPE A	120.3	24
o-DPE B	45.5	9
o-DPE C	110.7	22
M2-DPE	148.9	30
M2-DPE-A	200.5	40
M2-DPE-B	140.5	28
M4-DPE	41.3	8
o-M4-DPE A	170.5	34
o-M4-DPE B	285.1	57

4.3.4   Stability of diphenylethane autoxidation products and reactivity with glutathione

After isolation of the autoxidation products for DPE, M2-DPE and M4-DPE we investigated the ability of the compounds to react with reduced glutathione (GSH). GSH is commonly used for trapping of quinones and this experiment was designed to confirm which of the autoxidation products could form reactive quinones via autoxidation [14]. GSH formed adducts with o-DPE A, o-DPE C, o-M2-DPE B, o-M4-DPE A and o-M4-DPE B, but not with the fully aromatized compounds o-DPE B and o-M2-DPE A (Figure S13).

ESI (+) MS fragmentation of GSH adducts shows a neutral loss of 129 corresponding to pyroglutamic acid, which was observed for all of the GSH adducts. Since there is no exocyclic position for the GSH to react with the quinones, the GSH adducts should form on the ring which

subsequently re-aromatizes [28]. ESI (-) MS fragmentation of ring-adducted GSH produces a diagnostic fragment ion at *m/z* 272 indicating scission of the S-CH$_2$ bond of GSH; this diagnostic fragment ion was present for all of the adducts.

Additionally, we also determined that the cyclized diphenylethanes were unstable in the phosphate buffer over time (Table 3), except for the fully aromatized compounds o-DPE B and o-M2-DPE A. Both fully aromatized were stable in phosphate buffer up to 24 hours. It was also observed that o-DPE A oxidizes to o-DPE B.

Table 3. Oxidation rates of cyclized diphenylethanes (n=3) in phosphate-citric acid buffer (pH 7.4) at 37 ºC

Compound	k_{dep} (min^{-1})	$t_{1/2}$ (min)
o-DPE A	$1.3 \times 10^{-2} \pm 0.0010$	50
o-DPE C	$3.2 \times 10^{-2} \pm 0.0038$	21
o-M2-DPE B	$8.9 \times 10^{-3} \pm 0.0004$	77
o-M4-DPE A	$5.4 \times 10^{-3} \pm 0.0003$	128
o-M4-DPE B	$4.9 \times 10^{-3} \pm 0.0004$	141

4.4 Inhibition of *in vitro* α-synuclein aggregation

Thioflavin T (ThT) assay was used to determine the effect of the diphenylethanes and their oxidized products on the *in vitro* aggregation of α-synuclein. We measured the fluorescence at a single time point by incubating the test compounds with the protein for 5 days. Negative controls containing no drug were used to obtain an aggregated fluorescent response and were normalized to 100% of ThT fluorescence. We used cyclized nordihydroguaiaretic acid (cNDGA) as our positive control as it has been shown to inhibit the aggregation of α-synuclein in ThT assays [15]. Graphs containing ThT fluorescence results of different diphenylethanes and oxidized products are presented in Figure 11, and we normalized the readings averages and compared to controls/concentrations in Table 4.
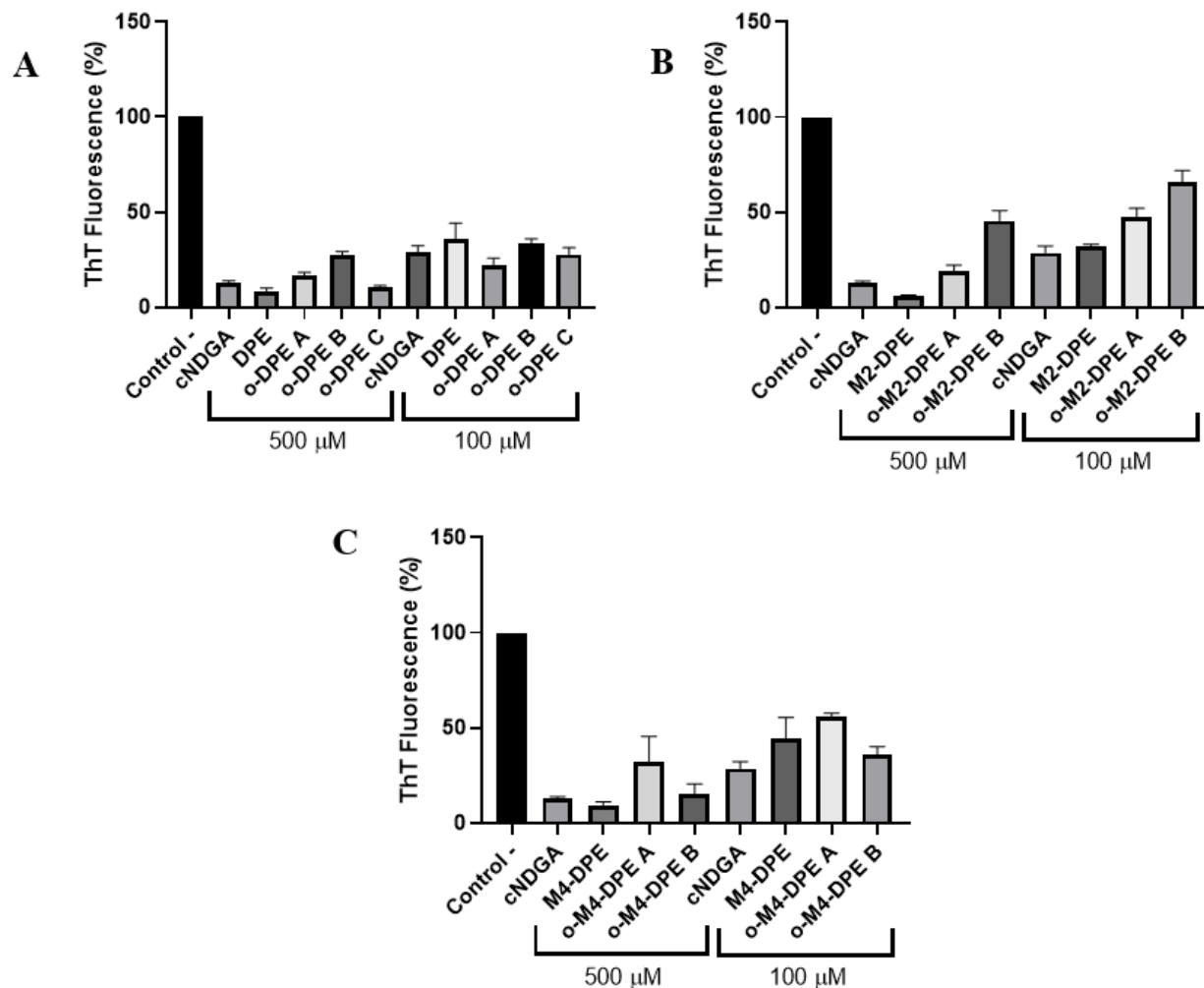
Figure 11. α-Synuclein aggregation represented as thioflavin T fluorescence percentage of positive control. Compounds are grouped in three panels according to their structures: DPE and o-DPEs (panel A), M2-DPE and o-M2-DPEs (panel B), and M4-DPE and o-M4-DPEs (panel C). All compounds were run in triplicate.

Table 4. *In vitro* activity of diphenylethanes (n=3) and their oxidized products (n=3) on α-synuclein aggregation.

Compound	α-Synuclein aggregation (%)	
	100 μM	**500 μM**
Control - (no drug)	100 [b]	100 [b]
Control + (cNDGA)	28.6 ± 3.6 [a]	13.6 ± 2.3 [a]
DPE	35.6 ± 8.5 [a]	8.1 ± 1.8 [a]
o-DPE A	22.2 ± 3.4 [a]	16.8 ± 1.4 [a]
o-DPE B	33.6 ± 2.3 [a]	25.9 ± 1.3 [a]
o-DPE C	27.8 ± 3.5 [a]	10.7 ± 0.5 [a]
M2-DPE	31.8 ± 1.3 [a]	6.1 ± 0.3 [a,c]
o-M2-DPE A	47.3 ± 4.8 [a,b]	19.3 ± 3 [a]
o-M2-DPE B	66.1 ± 5.8 [a,b]	45.6 ± 5.3 [a,b,c]
M4-DPE	44.4 ± 11 [a]	9.2 ± 1.9 [a]
o-M4-DPE A	56.1 ± 1.5 [a,b]	39.8 ± 1.6 [a]
o-M4-DPE B	36.1 ± 3.9 [a]	15.5 ± 4.9 [a]

[a] indicates a compound is statistically significant ($p < 0.05$) compared to the control –
[b] indicates a compound is statistically significant ($p < 0.05$) compared to the positive control at the same concentration
[c] indicates a compound is statistically significant ($p < 0.05$) comparing 100 μM to 500 μM

5. Discussion

The formation of intramolecular cyclized lignans such as cNDGA as a result of autoxidation in aqueous solution was previously discovered by our group [13] although many examples of similar cyclized lignans, for example the schisandrins [29], are known to occur in plants. In the case of NDGA, many *in vitro* studies have been carried out under conditions that would be expected to result in autoxidation occurring on a time scale shorter than the *in vitro* experiment, potentially confounding the results. Indeed, we have demonstrated that oxidation of NDGA or cNDGA is responsible for the inhibition of α-synuclein aggregation *in vitro* [15]. The intriguing observation that methyl substitution on the alkyl linker of NDGA decreased the rate of intramolecular cyclization [14] is opposite to that predicted for a vicinal dimethyl effect [30]. This observation led us to speculate whether di-catechol intramolecular autoxidative cyclizations occurred for other alkyl linker lengths and if this reversed vicinal dimethyl effect also occurred in diphenyl ethane-type di-catechols.

In our study we determined that our di-catechol substituted diphenylethane analogs underwent autoxidation to form dibenzocyclohexadienes 10-30 times more rapidly than dibenzocyclooctadienes formed from NDGA but, contrary to NDGA cyclization, the diphenylethanes autoxidized to intramolecular cyclization products at a rate that was proportional to the number of methyl substituents on the alkyl linker. The increase in rate of cyclization from DPE to M2-DPE (rate increase of 2.6 for O_2 purged) and from M2-DPE to M4-DPE (rate increase of 2.6 for O_2 purged) follows the same trend as observations of a vicinal dimethyl effect reported for lactone cyclization [30]. The authors in that study observed that addition of vicinal methyl groups at the 3,4 positions to ethyl 4-hydroxybutanoate resulted in an increase in cyclization rate of at least 5.3 and addition of gem dimethyl groups at the 3,3' position resulted in an increase in

cyclization rate of 4.4. Our results indicate that both vicinal and gem dimethyl effects may contribute to enhanced cyclization for the diphenylethanes.

We had previously proposed that the NDGA autoxidative cyclization was likely the result of a radical-mediated process [13] which was supported through subsequent *in silico* studies by Galano [31]. The dependence of cyclization in this study on oxygen in the buffer solution would indicate a similar radical mechanism. In our autoxidation study of NDGA, C-C bond formation occurred exclusively *para* to the 3-hydroxy group of the catechol. We observed however that for all of our diphenylethane analogs a mixture of regioisomers was formed. In addition to C-C bond formation occurring *para* to the 3-hydroxy group (o-DPE A, o-DPE B, o-M2-DPE A, o-M4-DPE A), we also observed C-C bond formation between the position *para* to the 3-hydroxy group of one ring with the position *ortho* to the 3-hydroxy group of the second ring (o-DPE C, o-M2-DPE B, o-M4-DPE B), presumably occurring through a process as outlined in Figure 12 for o-DPE C. It is possible that a small amount of the *ortho* 3-hydroxy regioisomer was formed however we were unable to detect this product. Additionally, we have determined that the relative amount of symmetrical cyclization was higher for DPE and M2-DPE, whereas relative amounts of asymmetrical cyclization was higher for M4-DPE (Table 2) although these differences are not large.
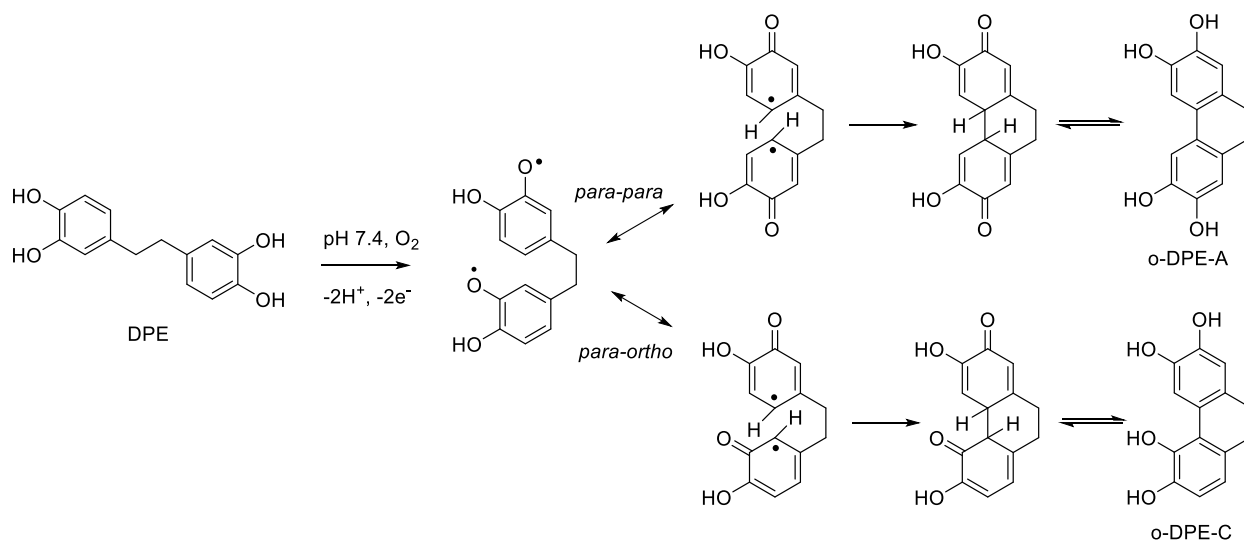
Figure 12. Proposed autoxidation mechanism of DPE to yield symmetrical (o-DPE A) and asymmetrical (o-DPE C) products

Our results led us to wonder why we do not observe a third regioisomer for C-C bond formation between the positions *ortho* to the 3-hydroxy groups on the diphenylethanes and why is the *ortho-para* mixed product not observed for NDGA cyclization. The aromatic rings are free to rotate in both NDGA and the diphenyethanes although the closer proximity of the rings in the diphenylethanes may result in H-bonding interactions although that may be anticipated to favour the *ortho-ortho* product which we did not observe. Alsoufi *et al* [32] carried out a Density Functional Theory (DFT) study which determined that biphenyl compounds resulting from phenoxyl radical coupling of catechols occurred preferentially in the order *para-para* followed by the mixed *para-ortho* and finally the *ortho-ortho* product, which is in agreement with our observations for the DPE and M2-DPE autoxidation products. The results reported by Alsoufi *et al* depicted the biphenyls in the lowest energy conformation with OH or C=O groups on opposite sides of the rings as shown for the keto-enol forms of the biphenyls (Figure 13). It should be noted that for our cyclized compounds the lowest energy conformations described by Alsoufi *et al* (Figure 13) cannot be

attained as the biphenyl bond cannot rotate the OH and C=O groups in the same manner due to the alkyl linker. The 10-30 fold slower rate of NDGA oxidation compared to DPE leading to greater selectivity for the more stable *para-para* cyclization product observed exclusively with NDGA is in line with the observations of Alsoufi *et al*. Curiously, we were unable to observe an aromatic autoxidation product for the asymmetric cyclization products o-DPE C and o-M2-DPE B however, we were also unable to find evidence of this structure in the literature.
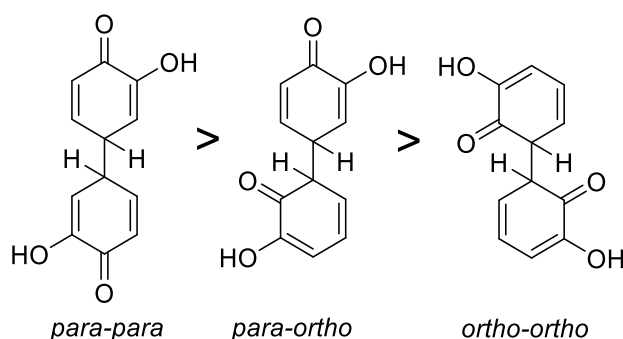
Figure 13. From the lowest to the highest energy conformation of biphenols resulting from phenoxyl radical coupling of catechols

We had previously observed that the rate of autoxidation of the cyclized NDGA compounds was more rapid than the initial autoxidation to the cyclized species [14]. For the DPE's however we observed that the cyclized products underwent further autoxidation at a slower rate than formation of the initial cyclized product and the *para-ortho* compounds o-M2-DPE B and o-M4-DPE B autoxidized slower than the corresponding *para-para* compounds. The only exception was the precursor of o-M2-DPE A, which we assume to be the cyclized, non-aromatized compound that we were unable to observe or isolate as it autoxidized to the aromatic species nearly instantaneously. The influence of methyl substituents on autoxidation rate of the cyclized compounds is variable, suggesting an electron-donating effect is unlikely.

While we were able to detect and isolate both the cyclized *para-para* non-aromatized product arising from DPE (o-DPE A) and the cyclized *para-para* aromatized product (o-DPE B), we were unable to detect or isolate the cyclized *para-para*, non-aromatized product arising from M2-DPE, instead only observing the cyclized *para-para* aromatized product (o-M2-DPE A). Evidently the cyclized *para-para*, non-aromatized M2-DPE product is highly unstable under these autoxidative conditions although it is not abundantly clear why. For the *meso* isomer of o-M2-DPE the gain in stabilization going from the twisted 6-membered ring with eclipsed vicinal methyl groups to the planar aromatic species may drive the reaction. For the racemic isomers the methyl groups could be in either a di-axial or di-equatorial conformation, but only the higher energy di-equatorial conformation may be expected to benefit from stabilization derived from aromatization.

Previously we have reported that NDGA and two cyclized analogs of NDGA inhibited α-synuclein aggregation [15] and others have reported that ethane di-catechol analogues inhibited α-synuclein aggregation *in vitro*. Based on these observations, we expected that our DPEs and their cyclized products would also show the same effect. Indeed, we observed a significant reduction ($p < 0.05$) in α-synuclein aggregation at both 100 and 500 μM. Even though only M2-DPE and o-M2-DPE B are statistically significant ($p < 0.05$) between the two concentrations tested, we observed a trend of concentration-dependent inhibition of α-synuclein for all compounds tested. Interestingly, both cyclized products of M2-DPE and one cyclized product of M4-DPE (o-M4-DPE A) significantly reduced ($p < 0.05$) the aggregation as compared to cNDGA at the same concentration. Our NDGA study indicated that the autoxidation process is required for the anti-aggregation effect and our DPE experiments agree with the earlier study.

In this study, we have prepared a series of 1,2-bis-ethane di-catechols to probe the influence of methyl substituents on intramolecular cyclization of di-catechols. We have determined that

these compounds undergo intramolecular cyclization to form dibenzocyclohexadienes and that steric interactions between the methyl substituents increased the rate of intramolecular cyclization. The cyclization of six-membered rings occurred 10-30 times more rapidly than formation of eight membered rings and both the DPEs and the dibenzocyclohexadienes prevent *in vitro* aggregation of α-synuclein. Our results strongly suggest that previously reported DPE analogs developed for the treatment of Parkinson's Disease likely owe their *in vitro* α-synuclein anti-aggregation activity to autoxidative processes.

6. Acknowledgments

7. References

1.   Parvathy KS, Negi PS, Srinivas P. Antioxidant, antimutagenic and antibacterial activities of curcumin-β-diglucoside. *Food Chem*. 2009;115(1):265-271.

2.   Apisariyakul A, Vanittanakom N, Buddhasukh D. Antifungal activity of turmeric oil extracted from *Curcuma longa* (Zingiberaceae). *J Ethnopharmacol*. 1995;49(3):163-169.

3.   Narlawar R, Pickhardt M, Leuchtenberger S, et al. Curcumin-Derived Pyrazoles and Isoxazoles: Swiss Army Knives or Blunt Tools for Alzheimer's Disease? *ChemMedChem*. 2008;3(1):165-172.

4.   Wang MS, Boddapati S, Emadi S, Sierks MR. Curcumin reduces alpha-synuclein induced cytotoxicity in Parkinson's disease cell model. *BMC Neurosci*. 2010;11:57. doi:10.1186/1471-2202-11-57

5.   Funk JL, Oyarzo JN, Frye JB, et al. Turmeric extracts containing curcuminoids prevent experimental rheumatoid arthritis. *J Nat Prod*. 2006;69(3):351-355. doi:10.1021/np050327j

6.   Shen L, Ji H-F. The pharmacology of curcumin: is it the degradation products? *Trends Mol Med*. 2012;18(3):138-144.

7.   Pan M-H, Huang T-M, Lin J-K. Biotransformation of Curcumin Through Reduction and Glucuronidation in Mice. *Drug Metab Dispos*. 1999;27(4):486 LP - 494.

8.   Metzler M, Pfeiffer E, Schulz SI, Dempe JS. Curcumin uptake and metabolism. *BioFactors*. 2013;39(1):14-20.

9.   Luis PB, Boeglin WE, Schneider C. Thiol Reactivity of Curcumin and Its Oxidation Products. *Chem Res Toxicol*. 2018;31(4):269-276.

10.   Jitoe-Masuda A, Fujimoto A, Masuda T. Curcumin: From Chemistry to Chemistry-Based

Functions. *Curr Pharm Des*. 2013;19(11):2084-2092.

11. Krafczyk N, Heinrich T, Porzel A, Glomb MA. Oxidation of the Dihydrochalcone Aspalathin Leads to Dimerization. *J Agric Food Chem*. 2009;57(15):6838-6843.

12. Roginsky V, Alegria AE. Oxidation of tea extracts and tea catechins by molecular oxygen. *J Agric Food Chem*. 2005;53(11):4529-4535. doi:10.1021/jf040382i

13. Billinsky JL, Krol ES. Nordihydroguaiaretic Acid Autoxidation Produces a Schisandrin-like Dibenzocyclooctadiene Lignan. *J Nat Prod*. 2008;71(9):1612-1615.

14. Asiamah I, Hodgson HL, Maloney K, Allen KJH, Krol ES. Ring substitution influences oxidative cyclisation and reactive metabolite formation of nordihydroguaiaretic acid analogues. *Bioorg Med Chem*. 2015;23(21):7007-7014.

15. Daniels MJ, Nourse JB, Kim H, et al. Cyclized NDGA modifies dynamic α-synuclein monomers preventing aggregation and toxicity. *Sci Rep*. 2019;9(1):2937.

16. Kim WS, Kågedal K, Halliday GM. Alpha-synuclein biology in Lewy body diseases. *Alzheimers Res Ther*. 2014;6(5):73.

17. Recasens A, Dehay B. Alpha-synuclein spreading in Parkinson's disease. *Front Neuroanat*. 2014;8:159.

18. Boston-Howes W, Williams EO, Bogush A, Scolere M, Pasinelli P, Trotti D. Nordihydroguaiaretic acid increases glutamate uptake in vitro and in vivo: Therapeutic implications for amyotrophic lateral sclerosis. *Exp Neurol*. 2008;213(1):229-237.

19. Ono K, Hasegawa K, Yoshiike Y, Takashima A, Yamada M, Naiki H. Nordihydroguaiaretic acid potently breaks down pre-formed Alzheimer's β-amyloid fibrils *in vitro*. *J Neurochem*. 2002;81(3):434-440.

20. Snow A, Nguyen B, Castillo G, et al. Compounds, Compositions and Methods for the

Treatment of Amyloid Diseases and Synucleinopathies such as Alzheimer's Disease, Type 2 Diabetes, and Parkinson's Disease. *WIPO WO2003101927A1*. Published online 2004.

21. Barrett TN, Braddock DC, Monta A, Webb MR, White AJP. Total Synthesis of the Marine Metabolite (±)-Polysiphenol via Highly Regioselective Intramolecular Oxidative Coupling. *J Nat Prod*. 2011;74(9):1980-1984.

22. Jung ME, Piizzi G. gem-Disubstituent Effect: Theoretical Basis and Synthetic Applications. *Chem Rev*. 2005;105(5):1735-1766.

23. Nwabufo CK, Aigbogun OP, Allen KJH, et al. Employing in vitro metabolism to guide design of F-labelled PET probes of novel α-synuclein binding bifunctional compounds. *Xenobiotica*. 2021;51(8):885-900.

24. Billinsky JL, Marcoux MR, Krol ES. Oxidation of the Lignan Nordihydroguaiaretic Acid. *Chem Res Toxicol*. 2007;20(9):1352-1358.

25. Tamaki K, Ishigami A, Tanaka Y, Yamanaka M, Kobayashi K. Self-Assembled Boronic Ester Cavitand Capsules with Various Bis(catechol) Linkers: Cavity-Expanded and Chiral Capsules. *Chem Eur J*. 2015;21(39):13714-13722.

26. Hartmann RW, Kranzfelder G, Von Angerer E, Schoenenberger H. Antiestrogens. Synthesis and evaluation of mammary tumor inhibiting activity of 1,1,2,2-tetraalkyl-1,2-diphenylethanes. *J Med Chem*. 1980;23(8):841-848.

27. Zeng W, Chemler SR. Total synthesis of (S)-(+)-tylophorine via enantioselective intramolecular alkene carboamination. *J Org Chem*. 2008;73(15):6045-6047.

28. Asiamah I, Krol ES. Quadrupole linear ion-trap mass spectrometry studies on glutathione conjugates of nordihydroguaiaretic acid (NDGA) analogues reveals phenol-type analogues are without reactive metabolite-mediated toxic liability. *Cogent Chem*.

2018;4(1):1562858.

29.   Szopa A, Ekiert R, Ekiert H. Current knowledge of *Schisandra chinensis* (Turcz.) Baill.

        (Chinese magnolia vine) as a medicinal plant species: a review on the bioactive

        components, pharmacological properties, analytical and biotechnological studies.

        Phytochem Rev. 2017;16(2):195-218.

30.   Brenna E, Dalla Santa F, Gatti FG, Gatti G, Tessaro D. Exploiting the vicinal disubstituent

        effect on the diastereoselective synthesis of γ and δ lactones. *Org Biomol Chem*.

        2019;17(4):813-821.

31.   Galano A, Macías-Ruvalcaba NA, Medina Campos ON, Pedraza-Chaverri J. Mechanism

        of the OH Radical Scavenging Activity of Nordihydroguaiaretic Acid: A Combined

        Theoretical and Experimental Study. *J Phys Chem B*. 2010;114(19):6625-6635.

32.   Alsoufi A, Altarawneh M, Dlugogorski BZ, Kennedy EM, Mackie JC. A DFT study on

        the self-coupling reactions of the three isomeric semiquinone radicals. *J Mol Struct

        THEOCHEM*. 2010;958(1):106-115.